Oceanologia 65 (2023) 398—409

Available online at www.sciencedirect.com

ScienceDirect

journal homepage: www.journals.elsevier.com/oceanologia

ORIGINAL RESEARCH ARTICLE

Seasonal variation in size structure and production of autotrophic plankton community in eutrophied, low-light environment: A focus on *Mesodinium rubrum*

Atis Labucis*, Astra Labuce, Iveta Jurgensone, Ieva Barda, Ingrida Andersone, Anda Ikauniece

Latvian Institute of Aquatic Ecology, Riga, Latvia

Received 10 July 2021; accepted 30 November 2022
Available online 11 December 2022

KEYWORDS
Primary production;
Coastal;
Brackish;
Gulf of Riga;
Baltic Sea;
Ciliate

Abstract Temporal variations in the primary production of the size-fractionated autotrophic plankton community were studied in coastal-estuarine waters of the eutrophic Gulf of Riga, Baltic Sea. The community was net-autotrophic during spring and summer and net-heterotrophic during autumn. The results of the present study clearly demonstrate strong co-variation between net primary production (NPP) and <56 μm fractionated community biomass, particularly small-sized (16—33 μm) *Mesodinium rubrum*, implying that the majority of NPP stems from the lower end of the size spectrum. A pronounced size distribution shift was observed within the *M. rubrum* population. Large-sized (length ≥ 34 μm) *M. rubrum* was the most abundant in the first half of the productive season (until week 24), whereas small-sized *M. rubrum* dominated during the stratified period.

1. Introduction

Mesodinium rubrum is a mixotrophic Litostomatea ciliate that possesses plastids preying upon cryptophyte algae (Hansen and Fenchel, 2006; Johnson et al., 2016). It is highly productive in turbid waters and at low light irradiance (Crawford, 1989; Herfort et al., 2012; Johnson and Stoecker, 2005; Moeller et al., 2011). *Mesodinium rubrum* is often abundant in estuarine-coastal waters (Cloern et al., 1994; Leles et al., 2017; Sanders, 1995), including the

* Corresponding author at: Latvian Institute of Aquatic Ecology, Voleru Str. 4, Riga, Latvia.
E-mail address: atis.labucis@lhei.lv (A. Labucis).
Peer review under the responsibility of the Institute of Oceanology of the Polish Academy of Sciences.

Production and hosting by Elsevier

https://doi.org/10.1016/j.oceano.2022.11.003

brackish Baltic Sea (Lips and Lips, 2017; Purina et al., 2018; Rychert, 2004). Additionally, under certain conditions, it forms blooms (red tides) (Taylor et al., 1971), yet *M. rubrum*-induced red tides are not reported from the temperate Baltic Sea region — the research area of the present study.

The main environmental factors promoting the growth and development of *M. rubrum* in temperate zones are season-specific (Johnson et al., 2013; Lips and Lips, 2017; Montagnes et al., 2008). Due to its motile abilities, *M. rubrum* benefits from strengthened stratification and the associated depletion of dissolved inorganic nutrients in the surface layers (Lips and Lips, 2017; Nishitani and Yamaguchi, 2018). Additionally, an elevated CO_2 concentration is not a hindrance to the successful development of *M. rubrum*; in contrast, Baltic *M. rubrum* increases its photosynthetic rate and forms a higher abundance under high-CO_2 treatment (Lischka et al., 2017). Thus, projected future climate change for the Baltic Sea region, (i.e., an increase in temperature, runoff and pH) and a decrease in salinity (BACC II, 2015; Havenhand, 2012; Omstedt et al., 2012), might expand the spatial and temporal space suitable for *M. rubrum* (Mitra et al., 2014). Considering the regional importance of *M. rubrum* in the Baltic Sea (Lips and Lips, 2017; Rychert, 2004), as well as its potential for expanded range and density in the future, it is essential to improve the knowledge base of *M. rubrum* ecology to better comprehend potential shifts in the functioning of the future Baltic Sea food web.

Mesodinium rubrum displays a wide size distribution (from 15 to 70 μm); therefore, size distinction is introduced in numerous studies on *M. rubrum* (e.g., Johansson, 2004; Johnson et al., 2016; Montagnes et al., 2008), revealing different ecological responses to environmental changes between size classes. Notably, *M. rubrum* has recently been recognised as a species complex consisting of at least two described and accepted species — *M. rubrum* and *Mesodinium major* (cf. Garcia-Cuetos et al., 2012; Johnson et al., 2016). Both have a similar morphology and possess plastids of the same origin (red plastid cryptophytes), but they show differences in cell length and ecology. *Mesodinium rubrum* cell length ranges between 16—35 μm, whereas longer cells are associated with *M. major*. In Danish waters of the Baltic Sea, *M. rubrum* is abundant during summer and early autumn, but *M. major* occurs mainly in the winter and early spring (Garcia-Cuetos et al., 2012). Recently, another *M. rubrum*-like species was identified in a Japanese brackish lake (Nishitani and Yamaguchi, 2018). It is seemingly morphologically identical to the *M. rubrum*/*major* complex but shows contrasting behaviour; it naturally preys upon green plastid cryptophytes. However, as molecular methods were not utilised in the present study, we refer to all *M. rubrum*-like ciliates as *M. rubrum*.

The estimates of planktonic primary production and identification of its main contributors are crucial to the comprehension of carbon flow dynamics and ecosystem functioning in general. The size and structure of the composition greatly influences the functioning of the pelagic food web (Lancelot and Muylaert, 2011; Tremblay and Legendre, 1994). Moreover, the recently proposed mixotrophic-centric paradigm for marine ecology highlights the need for detailed characterisation of mixotrophic functional groups (Mitra et al., 2014, 2016) to provide sufficient data for their inclusion within regional food web models. In the present study, we evaluated the contribution of *M. rubrum* to primary production in the eutrophic Gulf of Riga. To achieve this, we assessed the production of size-fractionated autotrophic communities, including small-sized (length of 16—33 μm) and large-sized *M. rubrum* (length ≥ 34 μm), and explored potential associations between production and seasonally changing environmental factors.

2. Material and methods

2.1. Study area

The Gulf of Riga (GoR) is a brackish semi-isolated area (16 330 km^2, 424 km^3; Berzinsh, 1995) of the Baltic Sea. It is connected to the Baltic Proper by narrow straits that confine water exchange. The shallowness of the GoR (average depth of 26 metres; Kotta et al., 2008) ensures the development of pronounced seasonal thermal stratification during the summer (Kotta et al., 2008). The mean salinity of the GoR ranges between 5 and 7 PSU, but it has a decreasing southward salinity gradient as the majority (approximately 86%) of the riverine runoff inflows into the southern part of the GoR (Berzinsh, 1995). Therefore, the southern GoR is characterised by higher water turbulence and increased values of riverine export (e.g., nutrients, suspended and dissolved organic matter, and chromophoric dissolved organic matter) that result in decreased water transparency. The study site (Figure 1) was located in the southern GoR to explore the habitat most suitable to *M. rubrum* within the GoR and thus evaluate the maximal potential effect *M. rubrum* may have on local primary production.

2.2. Sampling

Sampling was conducted at a national monitoring station (101A; Figure 1) located approximately 5 km from the mouth of the Daugava River. Samples were collected from 20 March 2017 to 24 October 2017 (Table 1) between 8 am and 10 am.

Water temperature and salinity were measured using a water probe (SBE 19plus Sea-Cat, USA). Photosynthetically active radiation (PAR) was measured using a LI-COR Data Logger equipped with an LI-190R Quantum Sensor. Water transparency was measured with a Secchi disc. Samples for estimating the concentration of nutrients (dissolved inorganic nitrogen (DIN): ammonium (NH_4^+), nitrate (NO_3^-), nitrite (NO_2^-); dissolved inorganic phosphorus (DIP): phosphate (PO_4^{3-}); dissolved silica (DSi): silicate (SiO_4^-)), phytoplankton community parameters (abundance, biomass) and primary production were obtained from the upper layer (0—10 m) using an integrated hose (inner diameter 25 mm) following HELCOM COMBINE Monitoring Guidelines (HELCOM, 2017). Nutrient concentrations were determined according to Grasshoff et al. (1983) (for a detailed description, see Purina et al. (2018)). All laboratory analyses were performed in an accredited laboratory (ISO/IEC 17205).

Integrated samples for phytoplankton analysis and estimation of primary production were divided into two types

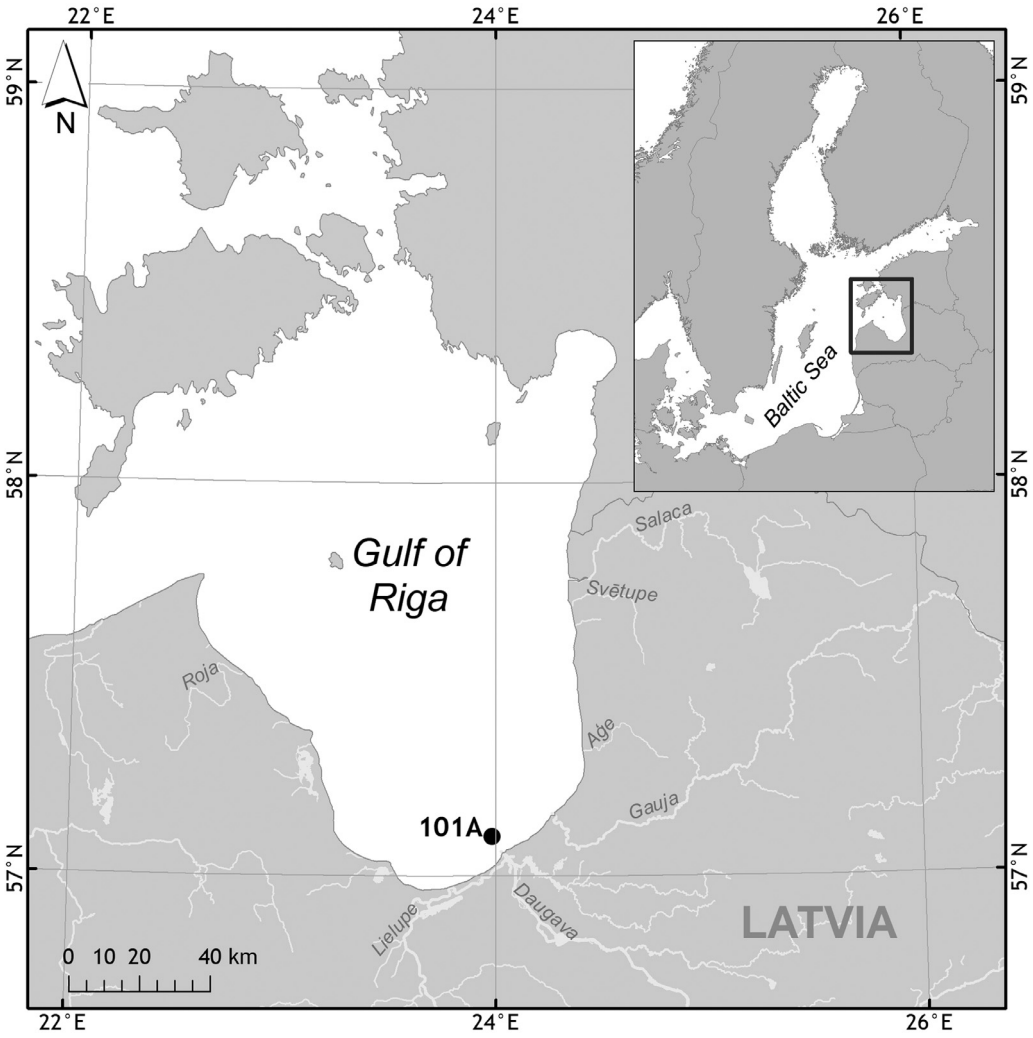

Figure 1 The location of sampling Station 101A (coordinates 57.10°N 23.98°E; depth approx. 22 m) in the Gulf of Riga.

(unfractionated and fractionated <56 μm) immediately after sampling. A size-fractionated approach has been widely used to extend the understanding of phytoplankton dynamics, as cell size directly affects responses to environmental variations (Malone and Chervin, 1979; Sin, 2000; Soria-Píriz et al., 2017) and associated impacts on the food web, e.g., via production (Cotti-Rausch et al., 2020; Mousseau et al., 1998; Probyn, 1990). The phytoplankton samples were divided by reverse fractionation: passed through a sieve with a mesh size of 56 μm (henceforth: <56-fractionated). The 56 μm sieve was chosen for fractionation based on the observed distribution of *M. rubrum* size classes in the long-term data collected at Station 101A (see database https://latmare.lhei.lv/).

Phytoplankton samples (300 ml) were fixed with acid Lugol's solution (final conc. 0.5%). Subsamples of 10 and 25 ml of fixed samples were settled in a sedimentation chamber for 8 and 18 hours, respectively, and counted according to the Uthermöl technique with an inverted microscope (Leica DMI 3000, Leica Microsystems GmbH, Germany) at 200x and 400x magnification. The number of counted cells in all subsamples exceeded 500 (HELCOM 2017; Olenina et al., 2006; Utermöhl, 1958). Both groups of samples (unfractionated and <56-fractionated) were handled identically during the analysis. Phytoplankton organisms were identified to the lowest possible taxonomic rank. Their names and classification complied with the accepted binomial nomenclature of the World Register of Marine Species (version 2021). Classification of *M. rubrum* into size classes >34 μm and 16–33 μm was based on the maximum cell dimension (HELCOM PEG biovolume file at https://helcom.fi/helcom-at-work/projects/peg/) and considering thresholds applied in other studies conducted in the Baltic Sea region (33 μm; Johansson, 2004). The biomass was expressed as gC m^{-2}. The carbon content was calculated according to Menden-Deuer and Lessard (2000).

2.3. Primary production measurements

Primary production rates were determined for each type of phytoplankton sample (unfractionated and <56-fractionated) separately. The light and dark bottle oxygen technique was used (Bender et al., 1987; Olesen et al., 1999) to evaluate the primary production of the study site. Fifteen transparent, calibrated (approximately 100 ml) glass bottles were filled with water for oxygen measure-

Table 1 Measurements of environmental variables in the upper 10 m layer at the sampling location (Station 101A) in the Gulf of Riga during 2017. PO_4 — dissolved inorganic phosphate, μmol l^{-1}; SiO_4 — dissolved silicate, μmol l^{-1}; NO_2 — nitrite, μmol l^{-1}; NO_3 — nitrate, μmol l^{-1}; NH_4 — ammonium, μmol l^{-1}; Secchi — water transparency depth, m; Temp — temperature, °C; Sal — salinity, PSU; PAR — photosynthetically active radiation, mol photons m^{-2} d^{-1}. * — observations not included in the PLSR.

	Week	PO_4^{3-}	SiO_4^-	NO_2^-	NO_3^-	NH_4^+	Secchi*	Temp	Sal	PAR
20-Mar	12	1.40	66.2	0.49	64.51	3.6	1.5	2.3	4.5	44
29-Mar	13	1.04	54.1	0.40	58.40	1.2	1	4.0	4.0	62
04-Apr	14	0.93	55.8	0.46	49.74	0.6	1.1	5.6	4.4	207
18-Apr	16	0.49	18.3	0.50	27.20	0.6	1.4	5.9	5.3	132
24-Apr	17	0.26	4.5	0.43	19.57	0.1	1.5	6.7	5.1	39
23-May	21	0.05	6.2	0.17	6.03	0.5	1.8	15.0	5.4	163
06-Jun	23	0.09	3.3	0.04	1.84	0.3	1.5	16.0	5.4	337
15-Jun	24	0.09	2.7	0.04	0.39	0.26	1.5	16.6	4.6	347
28-Jun	26	0.15	2.9	0.02	0.34	1.5	1.8	18.0	4.7	305
06-Jul	27	0.07	7.5	0.08	1.02	0.4	1.5	17.2	4.8	254
13-Jul	28	0.09	2.7	0.08	1.02	0.2	1.5	17.2	4.8	76
19-Jul	29	0.11	5.1	0.02	0.18	1.2	2.5	18.5	4.8	152
09-Aug	32	0.20	12.0	0.12	3.43	0.4	2.5	19.3	4.4	266
21-Aug	34	0.14	10.8	0.06	1.81	0.4	2.5	18.9	4.6	142
11-Sep	37	0.57	25.7	0.16	7.63	0.4	1.6	15.6	4.7	86
20-Sep	38	0.59	26.8	0.14	6.74	0.9	1.2	13.5	4.1	150
28-Sep	39	0.68	33.6	0.23	9.77	1.4	1.2	13.6	4.7	139
17-Oct	42*	NA	NA	NA	NA	2.2	1.9	10.6	4.1	29
25-Oct	43*	NA	NA	NA	NA	0.9	2.0	6.8	4.6	82

ments for both unfractionated and <56-fractionated samples (30 bottles in total). Bottles were divided into 5 groups with 3 replicates in each group for both sample types. One group of samples was set as an initial state, and the oxygen concentration was fixed with Winkler reagents (1 ml manganese chloride and 1 ml alkaline iodide) prior to incubation. The other four groups were incubated for 24 hours under conditions imitating light transmittance at specific depths of the euphotic layer: 100%, 66%, 23% and 0% light transmittance. To achieve these conditions, we wrapped the bottles in plastic optical filters (GAMPRODUCTS, Inc.) accordingly: no filter for 100% transparency, 1514 GAM for 66% transparency, 1516 GAM for 23% transparency and aluminium folium for 0% transparency. All vials used in the incubation were mounted on a rotating wheel and submerged in the onboard incubator with a continuous flow of seawater to ensure the ambient water temperature and *in situ* illumination during the 24-hour incubation. Every incubation was started approximately at the same time - between 11 am and 1 pm. After 24 hours, the samples were fixed with Winkler reagents. Oxygen concentrations were determined by titration with sodium thiosulfate according to ISO 5813:1983.

Oxygen consumption in the dark bottles (0% light transmittance) was used as a proxy of community respiration, while the other three groups (100%, 66%, and 23% light transmittance) were used to evaluate daily net primary production rates in the water column. The measured oxygen concentrations were converted to carbon units according to the stoichiometry of the photosynthesis equation (the conversion factor from ml O_2/l to gC/m^3 was 0.5357) (Bender et al., 1987; Van Niel, 1949). The approximate attenuation coefficient (k) was calculated for each sampling from Secchi depth (D_s) as:

$$k = 1.7/D_s.$$

The depth of specific light conditions (z) was calculated from:

$$z = -\frac{ln\left(\frac{I_z}{I_0}\right)}{k}$$

where I_z is the light intensity at a specific depth (66% or 23%) and I_o is the light intensity below the surface (100%). The daily net primary production rate (NPP, gC m^{-2} d^{-1}) was estimated by trapezoidal integration of the data from various light conditions. Gross primary production (GPP, gC m^{-2} d^{-1}) was calculated by summing NPP and respiration (gC m^{-2} d^{-1}). Annual gross primary production was calculated as the GPP monthly averages multiplied by the number of days and summed up for 365 days, assuming that production occurs only during the productive season, neglecting the period from November to February.

2.4. Statistical analysis

Data visualisation and analysis were performed using R software v.3.6.1 (R Core Team 2019; Wickham, 2009). A comparison of NPP between the unfractionated community and <56-fractionated community was conducted by the Wilcoxon signed-rank test.

The correlation between the primary production rates (NPP, GPP) and environmental variables was obtained by applying a partial least squares regression (PLSR). PLSR was performed using the functionality of the 'pls' package (Liland et al. 2022; Mevik and Wehrens, 2015) setting method to SIMPLS (De Jong, 1993). PLSR is a regression-like

technique which can handle the multi-collinearity issue and variables that are not normally distributed.

The importance of each explanatory variable in the PLSR model was estimated by the procedure of the Variable Importance for the Projection. Variable importance (expressed in percentage) was calculated based on weighted sums of the absolute regression coefficients by applying *varImp* function from the 'caret' package (Kuhn, 2021). The weights were calculated separately for each outcome as a function of the reduction of the sums of squares across the number of PLSR components. Prior to PLSR analysis, carbon masses of phytoplankton groups were Hellinger-transformed and all variables were centred and scaled to unit variance.

Unfractionated and <56-fractionated communities were analysed separately. The last two observations (weeks 42 and 43) were not included in the PLSR analysis due to a lack of nutrient data.

3. Results

3.1. Size range of *Mesodinium rubrum*

A wide size range (16—65 μm in length; Figure 2) was observed in the *M. rubrum* population. The population was dominated by large (≥34 μm) specimens during the spring and by smaller *M. rubrum* in the following period. Average-sized cells (33—28 μm) were less prevalent; therefore, we established division into two groups — large-sized and small-sized. Cells 34 μm or longer were designated as large, while those under 34 μm were designated as small.

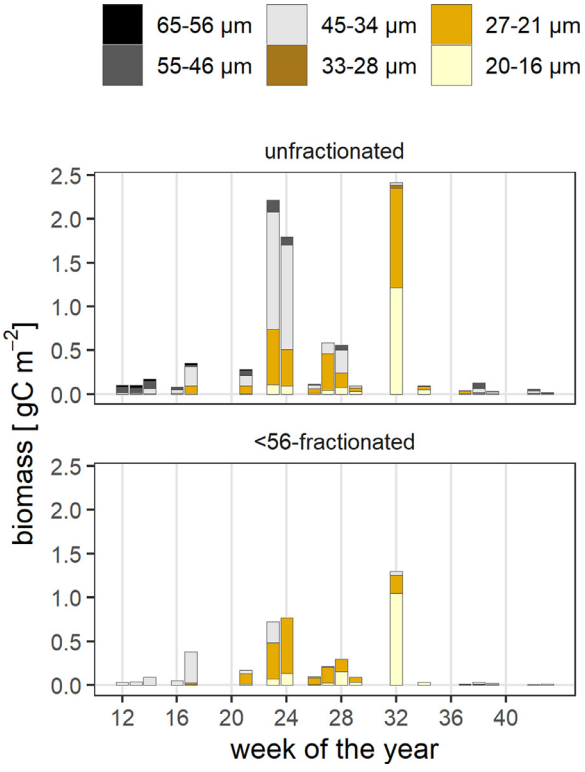

Figure 2 Dynamics of size classes within the *Mesodinium rubrum* population in an unfractionated and <56-fractionated phytoplankton community of the Gulf of Riga.

3.2. Environmental conditions: abiotic drivers

The temporal dynamics of the measured environmental parameters are shown in Table 1. Overall, environmental variables changed seasonally, with the highest temperature and lowest nutrient values during the summer. Salinity and water transparency varied marginally, whereas PAR intensity was mainly dependent on the season and cloud cover and varied considerably during the studied period.

3.3. Environmental conditions: phytoplankton population

The phytoplankton community showed a typical succession for temperate coastal waters during the study period (Figure 3). The highest total carbon mass (3.2—4.3 gC m^{-2}) within the unfractionated autotrophic community was observed in spring (weeks 16—17), when diatoms, mainly *Chaetoceros wighamii* and *Thalassiosira baltica*, prevailed. Diatoms were successively replaced by motile taxa, (i.e., the dinoflagellate *Peridiniella catenata* and the large-sized (≥34 μm) ciliate *M. rubrum*), which dominated the phytoplankton community until mid-June (week 24). *M. rubrum* contributed approximately 70% to the carbon mass of both the unfractionated and <56-fractionated communities during weeks 23—24.

Cyanobacteria and small-sized (16—33 μm) *M. rubrum* co-dominated during the summer period (weeks 26—32). The highest carbon mass of the cyanobacterium *Aphanizomenon flos-aquae* (1.66 gC m^{-2}) and small-sized *M. rubrum* (2.39 gC m^{-2}; 95% of total carbon mass) was observed in mid-July (week 28) and early August (week 32), respectively. Chlorophyceae (*Dictyosphaerium ehrenbergianum*, *Oocystis* spp., and *Raphidocelis sigmoidea*), Cryptophyceae (*Plagioselmis prolonga* and *Teleaulax* spp.), Prasinophyceae (*Pyramimonas* spp.) and Prymnesiophyceae (*Chrysochromulina* spp.) increased in carbon mass during the summer period (weeks 23—32), showing similar dynamics as cyanobacteria and small-sized *M. rubrum* (Figure 3).

The phytoplankton community in <56-fractionated samples showed an analogous succession pattern, except for large diatoms and filamentous cyanobacterium *A. flos-aquae*, which were filtered out during fractionation (Figure 3). Dinoflagellates (*Heterocapsa rotundata* and *P. catenata*) together with small-sized *M. rubrum* dominated the <56-fractionated community during spring when *M. rubrum* contributed up to 40% of the total carbon mass. A slight increase in Chlorophyceae (*D. ehrenbergianum* and *R. sigmoidea*), Cryptophyceae (*P. prolonga* and *Teleaulax* spp.) and Prasinophyceae (*Pyramimonas* spp.) was observed during cyanobacteria dominance (weeks 26—29). Notably, small-sized *M. rubrum* reached its maximum carbon mass soon afterward and compiled approximately 80% of the total carbon mass (week 32).

3.4. Primary production

The GPP and NPP of both the unfractionated and <56-fractionated autotrophic communities varied seasonally (Figure 4). Overall, the planktonic community was net autotrophic during spring and summer and net heterotrophic

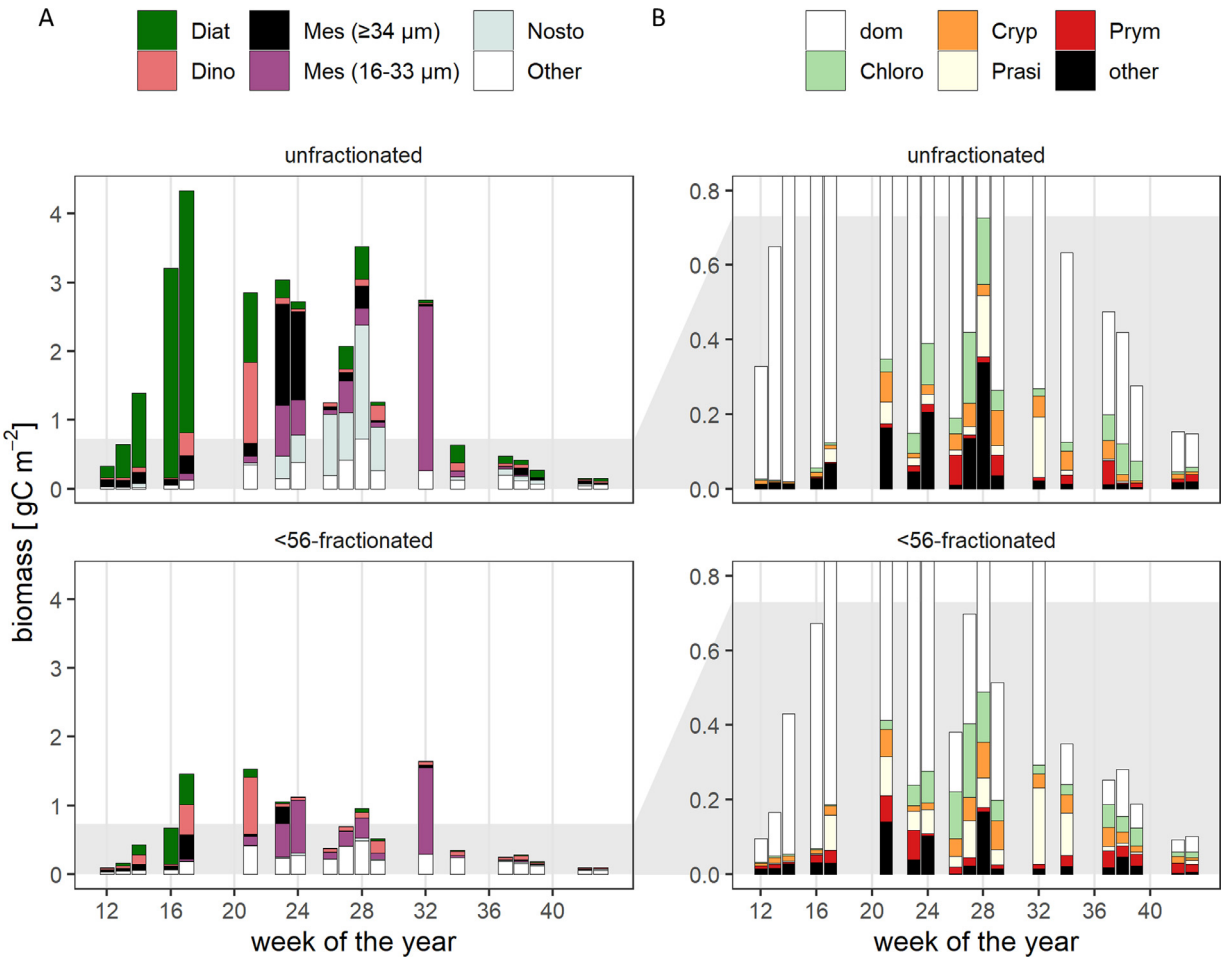

Figure 3 Temporal dynamics of A) dominant phytoplankton taxonomic groups and B) other phytoplankton taxonomic groups in unfractionated (upper) and 56-fractionated samples (lower) from the top 10 m layer at the sampling location (Station 101A) in the Gulf of Riga. Diat — Diatomophyceae; Dino — Dinophyceae; Mes (≥34 µm) — large-sized *Mesodinium rubrum*; Mes (16—33 µm) — small-sized *Mesodinium rubrum*; Nosto — Nostocophyceae/cyanobacteria; dom — dominant groups — shown in graph A; Chloro — Chlorophyceae; Cryp — Cryptophyceae; Prasi — Prasinophyceae; Prym — Prymnesiophyceae. Mind the differences in scales of Y-values, follow the grey area for rescaling.

during autumn (Figure 4A). The amount of both NPP and GPP of the unfractionated community was not significantly different from the amount produced by the <56-fractionated community (for NPP $V_{Wilcoxon} = 205.00$, $p = 0.488$, n = 19; for GPP $V_{Wilcoxon} = 194.00$, $p = 0.708$, n = 19). The only evident disparity was during the spring bloom (weeks 12 to 16), when the NPP of the <56-fractionated community was almost twice as low as the NPP of the unfractionated community. From week 17 to week 23, NPP increased from 0.04 to 0.53 gC m^{-2} d^{-1} and from 0.02 to 0.28 gC m^{-2} d^{-1} within the unfractionated and <56-fractionated communities, respectively (Figure 4A). Afterwards, a decrease in NPP was observed, dropping below 0 gC m^{-2} d^{-1} by week 29. The sampling events conducted in weeks 28 and 29 were characterised by low PAR values (Table 1), potentially causing a decrease in NPP values (Figure 4A).

3.5. Environmental conditions influencing primary production

The first two components of PLSR model explained 59.7% and 54.4% of the primary production (NPP, GPP) variance for unfractionated and <56-fractionated communities, respectively (Table 2, Figure 5). The results showed that NPP was influenced by fewer environmental factors than GPP (Figure 6). The analysis identified small-sized *M. rubrum* and PAR as the most important influencing parameters for NPP in both unfractionated and <56-fractionated communities (Figure 6A, C), whereas for GPP, besides small-sized *M. rubrum* and PAR, also nutrients, temperature, and carbon mass of diatoms were identified as important factors (Figure 6B, D).

4. Discussion

Surveys of primary production in the GoR have been sporadic in the last decades (Olesen et al., 1999; Wassmann and Tamminen, 1999; Wasmund et al., 2001), mainly covering the period from 1993 to 1997. More recently, the dynamics of primary production in the GoR were analysed in relation to seasonal changes in the phytoplankton community and nutrient concentrations (Labucis et al., 2017; Purina et al., 2018). However, the abovementioned studies focused on

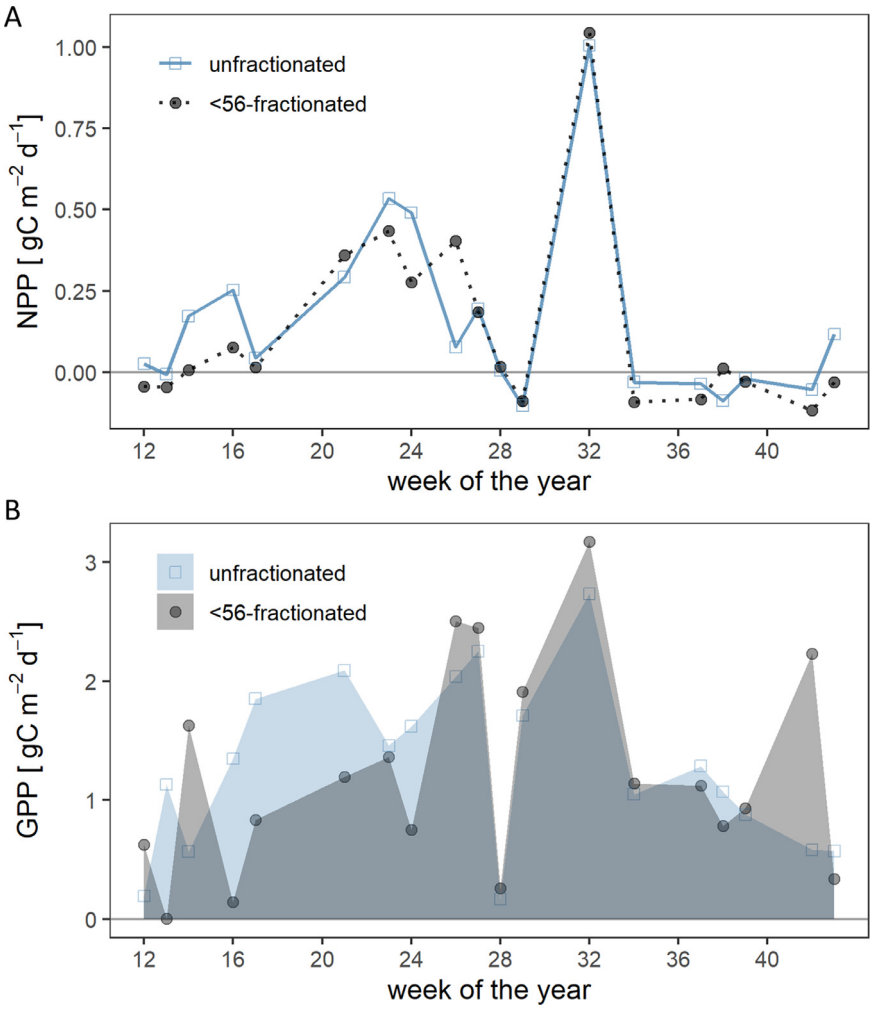

Figure 4 Average daily A) net primary production (NPP) and B) gross primary production (GPP) of unfractionated and <56-fractionated autotrophic communities from the top 10 m layer at the sampling location (Station 101A) in the Gulf of Riga.

Table 2 Results of partial least squares regression (PLSR). Comp — components; SS — the sum of squared loadings.

	Comp1	Comp2	Comp3	Comp4	Comp5
unfractionated					
SS loadings	3.79	1.42	0.993	0.57	0.50
Explained variance [%]	40.70	19.00	10.10	8.40	6.50
Cumulative Proportion [%]	40.70	59.70	69.80	78.20	84.70
<56-fractionated					
SS loadings	5.67	3.03	1.32	0.76	0.36
Explained variance [%]	42.50	11.90	13.40	7.60	9.00
Cumulative Proportion [%]	42.50	54.40	67.80	75.40	84.40

primary production by the unfractionated community. The present study is the first to analyse the production of the fractionated autotrophic community of the GoR.

Size fractionation is often used to separate phytoplankton communities into picoplankton, nanoplankton and microplankton (Fenchel, 1988); however, it is also a useful approach to investigating other size fractions of interest. The results of the present study clearly demonstrate strong covariation between NPP and <56-fractionated community taxa (Figure 4), particularly the small-sized (16—33 μm) *M. rubrum* (Figures 5—6). This implies that the majority of NPP stems from the lower end of the size spectrum. Size fractionation eases the pressure of light, space and nutrient limitation on smaller organisms, thus not only revealing their growth and production potential under experimental conditions (Sommer et al., 2016) but also confirming their impor-

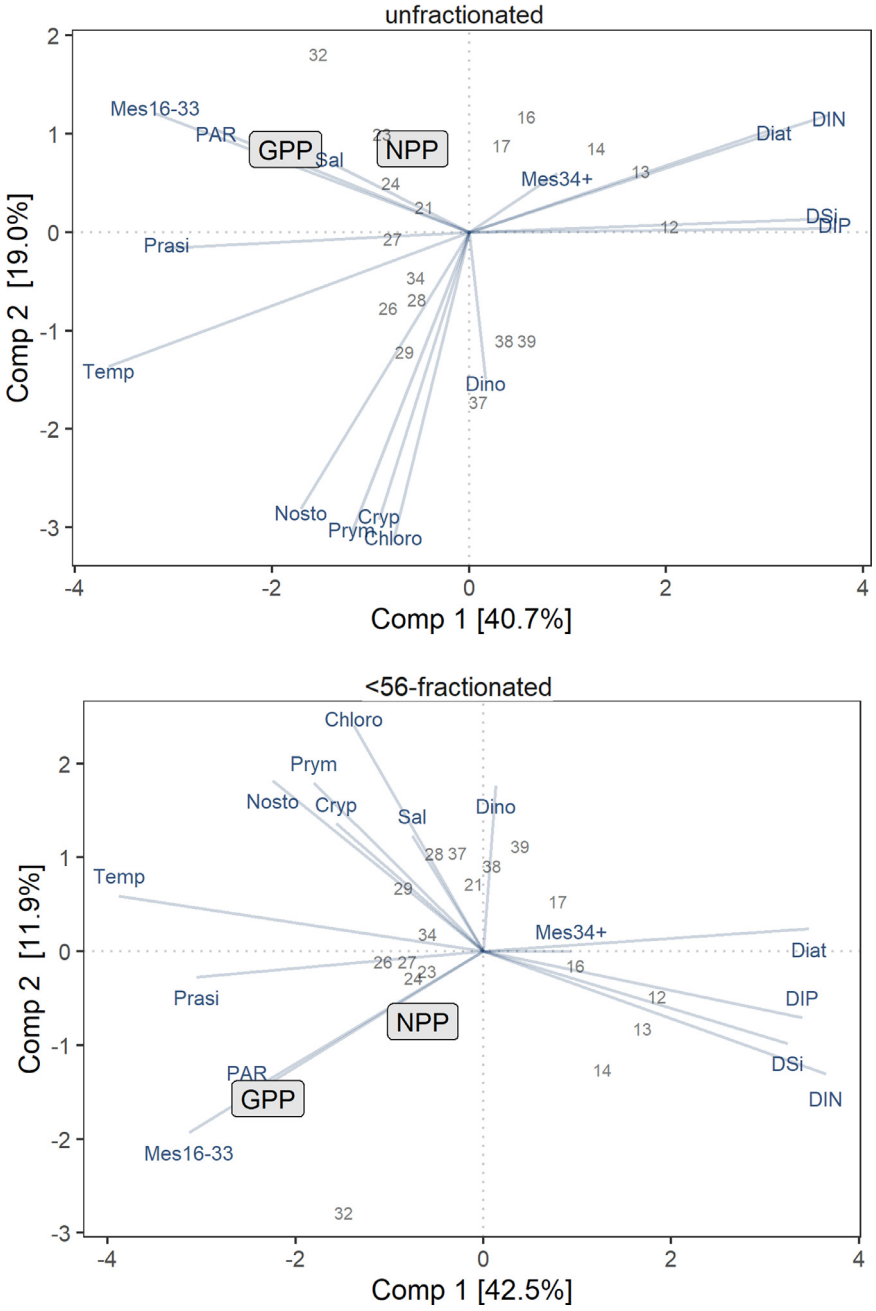

Figure 5 Partial least squares regression (PLSR) triplots associated to the first two components. PLSR performed between the primary production rates (NPP — net primary production; GPP — gross primary production) and environmental variables (DIN — dissolved inorganic nitrogen; DIP — dissolved inorganic phosphorus; DSi — dissolved silicate; PAR — photosynthetically active radiation; Sal — salinity; Temp — temperature; carbon mass of phytoplankton groups: Diat — Diatomophyceae; Dino — Dinophyceae; Mes34+ — large-sized (≥34 μm) *Mesodinium rubrum*; Mes16—33 — small-sized (16—33 μm) *Mesodinium rubrum*; Nosto — Nostocophyceae/cyanobacteria; Chloro — Chlorophyceae; Cryp — Cryptophyceae; Prasi — Prasinophyceae; Prym — Prymnesiophyceae). Primary production rates are represented as labels on a grey background; environmental variables are represented as solid navy-blue lines; sampling week (sites) are shown as grey numbers.

tance in the production of unfractionated samples. Small cells of primary producers have an advantage due to their larger surface-to-volume ratio that facilitates nutrient uptake compared to larger cells (Falkowski and Oliver, 2007).

Fractionation exposed unfractionated community as inefficient net-producers at the study site due to their high respiration rates (Figure 4). Notably, the respiration of the unfractionated community was high because it also included heterotrophic protozoans (e.g., tintinnids) and metazoans (e.g., rotifers and Copepoda nauplii). In general, respiration of microzooplankton is estimated to reach 35—43% on average of daily primary production (Calbet and Landry, 2004). Due to the size overlap, it was not possible to filter out zooplankton prior to incubation without also removing diatoms,

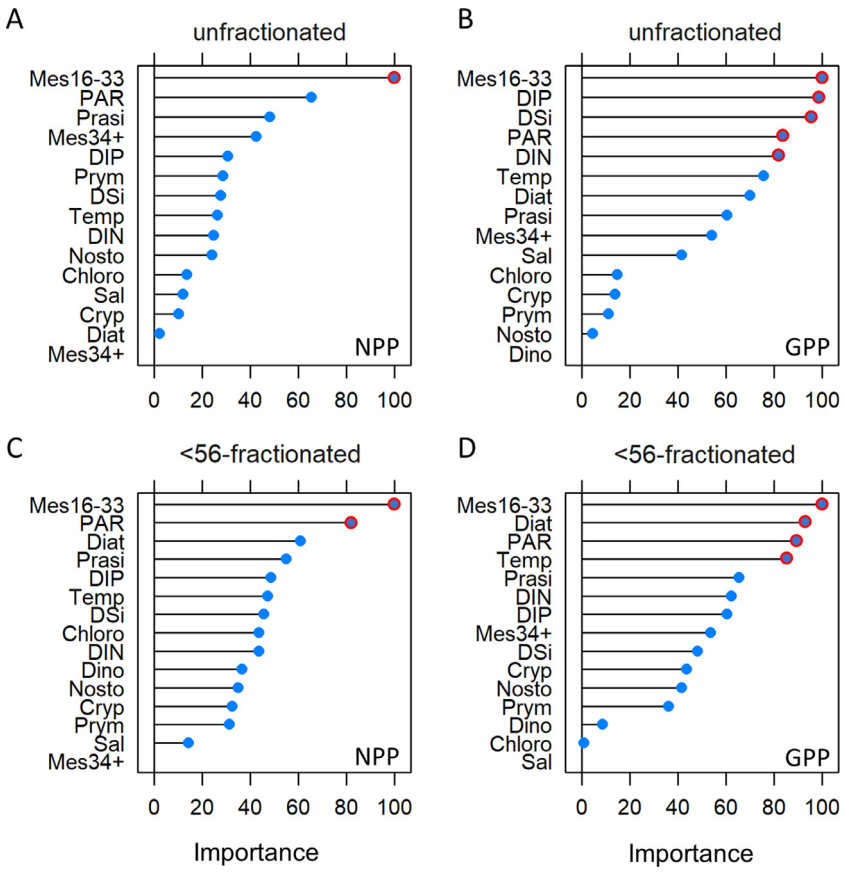

Figure 6 Variable importance for the projection (VIPs) for explanatory variables of partial least squares regression (PLSR) model. A) VIPs of NPP of unfractionated community, B) VIPs of GPP of unfractionated community, C) VIPs of NPP of <56-fractionated community, and D) VIPs of GPP of <56-fractionated community. The most influential variables (VIPs > 80%) are marked with red circles.

filaments of cyanobacteria, and dinoflagellates. Hence, the results of respiration (and GPP) should be interpreted with caution if compared to estimates obtained by a different method (i.e., other than the light-dark bottle oxygen technique).

The annual GPP of the unfractionated community in the present study was 8.5—14.1% lower (i.e., 323 gC m^{-2}) than that estimated for the central part of the GoR (Purina et al., 2018; GPP estimated using the same approach as in the present study). This is most likely a result of lowered water transparency due to coastal water turbulence and a direct impact of opaque freshwater discharge at the present study site. Indeed, Secchi depth varied between 2.3 and 5.1 m in the central part of the GoR (Purina et al., 2018), whereas it did not exceed 2.5 m in this study (southern coastal area). However, *M. rubrum* showed significant covariation to primary production rates in both areas (Purina et al., 2018; Figure 5) despite the different underwater light conditions expressing its flexible nature. Additionally, in several other Baltic subbasins, *M. rubrum* has been stated as a significant contributor to primary production (Höglander et al., 2004; Johansson, 2004; Lips and Lips, 2017; Nielsen and Kiørboe, 1994), implying its essential role as one of the main producers in the Baltic Sea.

Mesodinium rubrum is known to have migration behaviour based on the response of phototaxis (Crawford and Lindholm, 1997) and has wide temperature, salinity and light tolerances (Lindholm and Mörk, 1990; Olli et al., 1996). It can migrate vertically over tens of metres per day (Hajdu et al., 2007), exploiting the nutrient-rich lower layers. *Mesodinium rubrum* benefits from this behaviour under stratified conditions in the shallow Baltic Sea (Lips and Lips, 2017). Due to the focus on the surface layer in the present study, subsurface accumulations of motile phytoplankton are most likely missed, potentially resulting in an underestimate of the overall abundances and biomass of *M. rubrum*. However, the efficient production of *M. rubrum* is attributed to mixotrophy and photosynthetic machinery of cryptophyte-originated chloroplasts that are well adapted to dim light (Daneri et al., 1992; Herfort et al., 2012) rather than the ability of vertical migration. The photosynthetic activity of *M. rubrum* increases with the availability of cryptophytes, although with a 7-day lag (Gustafson et al., 2000). In general, mixotrophy is an advantage under nutrient-limited conditions (Mitra et al., 2014), and it is an important feeding strategy during the decline of spring blooms and during summer or other periods when the system shifts from net autotrophy to net heterotrophy (Haraguchi et al., 2018). However, the ecological flexibility of *M. rubrum* and its implications for its phototrophic production remain poorly understood and require further in-depth research.

Cryptophytes are common in the GoR during summer (Figure 3). Hence, the acquisition of chloroplasts does not limit the growth of *M. rubrum*, allowing it to reach the

highest efficiency in photosynthetic activity without notable limitations. Nevertheless, cryptophytes affect various aspects of the performance of *M. rubrum*. In addition to the aforementioned physiological components, the availability of *Teleaulax* cryptophytes reduces the average size and volume of *M. rubrum* cells, as the high prevalence of cryptophytes promotes cell division (Gustafson et al., 2000). A potential explanation for a shift to small-sized *M. rubrum* during summer in the GoR is that cryptophytes were the most abundant in the period between weeks 26 and 32. A shift from larger to smaller *M. rubrum* during summer has also been observed in other Baltic Sea regions. This is explained by increased grazing pressure (Johansson, 2004; Rychert, 2004; Witek, 1998), higher temperature (Garcia-Cuetos et al., 2012; Haraguchi et al., 2018), and low DIN values (Haraguchi et al., 2018) during the summer.

In line with future global projections, climate change scenarios for the GoR region foresee a continuation of already occurring air temperature and precipitation increases. A consequent drop in frost and ice days will follow (BACC II, 2015). Overall, the winters will become milder, but the summers will become more pronounced. The changes will promote stratification and inorganic nutrient (especially nitrogen) limitation in the surface layer, as well as potentially decrease the light availability even further (Skudra and Lips, 2017; Sommer et al., 2012; Winder and Schindler, 2004). Organisms with coping mechanisms to nutrient deficiency in the euphotic layer (e.g., motile *M. rubrum*, diazotrophic cyanobacteria) will outperform others under such conditions (Griffiths et al., 2016; Spilling and Markager, 2008; Wasmund and Uhlig, 2003). Moreover, future climate conditions appear non-detrimental to cryptophytes (Gaillard et al., 2020), thus predicting the continuous availability of cryptophyte-originated chloroplasts ensuring autotrophy of *M. rubrum*. Several studies have revealed that *M. rubrum* is able to remain photosynthetic and survive for months at low irradiance (Johnson and Stoecker, 2005) considering its efficient inorganic nutrient uptake rates (Stoecker et al., 1991; Tong et al., 2015; Wilkerson and Grunseich, 1990). Therefore, an increase in the prevalence of *M. rubrum*, along with a consequent rise in primary production, can be expected in the region, especially during the summer period.

Last, the present study demonstrated a close link between *M. rubrum* (especially small-sized *M. rubrum*) and NPP in coastal waters of the GoR (Figure 6). However, large-sized *M. rubrum* was coabundant with small-sized *M. rubrum* for a short period of time, soon after the spring bloom (Figure 2), limiting direct comparison between them. It is highly likely that the unequal amount of available PAR in spring and summer had a role in the identified different contributions to NPP between the size classes of *M. rubrum*.

Acknowledgements

We would like to warmly thank our colleagues Ņina Sunelika, Alla Ivakina and Miķelis Mazmačs for nutrient analysis and work onboard, as well as crews of r/v *Salme* and A-90 *Varonis*. We also thank the anonymous reviewers for their comments and Maija Leff for revising the English. The research was partly supported by the Latvian State research program EVIDEnT "The value and dynamic of Latvia's ecosystems under changing climate." The authors have no conflicts of interest to declare.

Declaration of competing interests

The authors declare that they have no known competing financial interests or personal relationships that could have appeared to influence the work reported in this paper.

References

BACC II, 2015. Second Assessment of Climate Change for the Baltic Sea Basin. Springer Int. Publ. https://doi.org/10.1007/978-3-319-16006-1

Bender, M., Grande, K., Johnson, K., Marra, J., Williams, P.J.L., Sieburth, J., Pilson, M., Langdon, C., Hitchcock, G., Orchardo, J., Hunt, C., Donaghay, P., Heinemann, K., 1987. A comparison of four methods for determining planktonic community production. Limnol. Oceanogr. 32, 1085—1098.

Berzinsh, V., 1995. Hydrology. Ecosystem of the Gulf of Riga between 1920 and 1990. Academia 5, 7—8.

Calbet, A., Landry, M.R., 2004. Phytoplankton growth, microzooplankton grazing, and carbon cycling in marine systems. Limnol. Oceanogr. 49, 51—57. https://doi.org/10.4319/lo.2004.49.1.0051

Cloern, J.E., Cole, B.E., Hager, S.W., 1994. Notes on a *Mesodinium rubrum* red tide in San Francisco Bay (California, USA). J. Plankton Res. 16, 1269—1276.

Cotti-Rausch, B.E., Lomas, M.W., Lachenmyer, E.M., Baumann, E.G., Richardson, T.L., 2020. Size-fractionated biomass and primary productivity of Sargasso Sea phytoplankton. Deep Sea Res. Pt. I 156, 103141. https://doi.org/10.1016/j.dsr.2019.103141

Crawford, D.W., 1989. *Mesodinium rubrum*: the phytoplankter that wasn't. Mar. Ecol. Prog. Ser. 58, 161—174.

Crawford, D.W., Lindholm, T., 1997. Some observations on vertical distribution and migration of the phototrophic ciliate *Mesodinium rubrum* (= *Myrionecta rubra*) in a stratified brackish inlet. Aquat. Microb. Ecol. 13, 267—274. https://doi.org/10.3354/ame013267

Daneri, G., Crawford, D.W., Purdie, D.A., 1992. Algal blooms in coastal waters: a comparison between two adaptable members of the phytoplankton, *Phaeocystis* sp. and *Mesodinium rubrum*. In: Vollenweider, R.A., Marchetti, R., Viviani, R. (Eds.), Marine Coastal Eutrophication. Elsevier, Amsterdam, 879—890. https://doi.org/10.1016/B978-0-444-89990-3.50076-6

De Jong, S., 1993. SIMPLS: an alternative approach to partial least squares regression. Chemometr. Intell. Lab. 251—263. https://doi.org/10.1016/0169-7439(93)85002-X

Falkowski, P.G., Oliver, M.J., 2007. Mix and match: how climate selects phytoplankton. Nat. Rev. Microbiol. 5, 813—819. https://doi.org/10.1038/nrmicro1751

Fenchel, T., 1988. Marine plankton food chains. Annu. Rev. Ecol. Syst. 19, 19—38.

Gaillard, S., Charrier, A., Malo, F., Carpentier, L., Bougaran, G., Hégaret, H., Réveillon, D., Hess, P., Séchet, V., 2020. Combined Effects of Temperature, Irradiance, and pH on *Teleaulax amphioxeia* (Cryptophyceae) Physiology and Feeding Ratio For Its Predator *Mesodinium rubrum* (Ciliophora). J. Phycol. 56, 775—783. https://doi.org/10.1111/jpy.12977

Garcia-Cuetos, L., Moestrup, Ø., Hansen, P.J., 2012. Studies on the genus *Mesodinium* II. Ultrastructural and molecular investigations of five marine species help clarifying the taxonomy.

J. Eukaryot. Microbiol. 59, 374—400. https://doi.org/10.1111/j.1550-7408.2012.00630.x
Grasshoff, P., Ehrhardt, M., Kremling, K., 1983. Methods of seawater analysis. Verlag Chemie, Weinheim, 419 pp.
Griffiths, J.R., Hajdu, S., Downing, A.S., Hjerne, O., Larsson, U., Winder, M., 2016. Phytoplankton community interactions and environmental sensitivity in coastal and offshore habitats. Oikos 125, 1134—1143. https://doi.org/10.1111/oik.02405
Gustafson Jr, D.E., Stoecker, D.K., Johnson, M.D., Van Heukelem, W.F., Sneider, K., 2000. Cryptophyte algae are robbed of their organelles by the marine ciliate *Mesodinium rubrum*. Nature 405, 1049—1052. https://doi.org/10.1038/35016570
Hajdu, S., Höglander, H., Larsson, U., 2007. Phytoplankton vertical distributions and composition in Baltic Sea cyanobacterial blooms. Harmful Algae 6, 189—205. https://doi.org/10.1016/j.hal.2006.07.006
Hansen, P.J., Fenchel, T., 2006. The bloom-forming ciliate *Mesodinium rubrum* harbours a single permanent endosymbiont. Mar. Biol. Res. 2, 169—177. https://doi.org/10.1080/17451000600719577
Haraguchi, L., Jakobsen, H.H., Lundholm, N., Carstensen, J., 2018. Phytoplankton Community Dynamic: A Driver for Ciliate Trophic Strategies. Front. Mar. Sci. 5. https://doi.org/10.3389/fmars.2018.00272
Havenhand, J.N., 2012. How will ocean acidification affect Baltic sea ecosystems? an assessment of plausible impacts on key functional groups. Ambio 41, 637—644. https://doi.org/10.1007/s13280-012-0326-x
HELCOM, 2017. Manual for Marine Monitoring in the COMBINE Programme of HELCOM. http://www.helcom.fi/action-areas/monitoring-and-assessment/manuals-and-guidelines/combine-manual
Herfort, L., Peterson, T.D., Prahl, F.G., McCue, L.A., Needoba, J.A., Crump, B.C., Roegner, G.C., Campbell, V., Zuber, P., 2012. Red Waters of *Myrionecta rubra* are Biogeochemical Hotspots for the Columbia River Estuary with Impacts on Primary/Secondary Productions and Nutrient Cycles. Estuaries Coasts 35, 878—891. https://doi.org/10.1007/s12237-012-9485-z
Höglander, H., Larsson, U., Hajdu, S., 2004. Vertical distribution and settling of spring phytoplankton in the offshore NW Baltic Sea proper. Mar. Ecol. Prog. Ser. 283, 15—27. https://doi.org/10.3354/meps283015
Johansson, M., 2004. Annual variability in ciliate community structure, potential prey and predators in the open northern Baltic Sea proper. J. Plankton Res. 26, 67—80. https://doi.org/10.1093/plankt/fbg115
Johnson, M.D., Beaudoin, D.J., Laza-Martinez, A., Dyhrman, S.T., Fensin, E., Lin, S., Merculief, A., Nagai, S., Pompeu, M., Setälä, O., Stoecker, D.K., 2016. The Genetic Diversity of *Mesodinium* and Associated Cryptophytes. Front. Microbiol. 7, 2017. https://doi.org/10.3389/fmicb.2016.02017
Johnson, M.D., Stoecker, D.K., 2005. Role of feeding in growth and photophysiology of *Myrionecta rubra*. Aquat. Microb. Ecol. 39, 303—312. https://doi.org/10.3354/ame039303
Johnson, M.D., Stoecker, D.K., Marshall, H.G., 2013. Seasonal dynamics of *Mesodinium rubrum* in Chesapeake Bay. J. Plankton Res. 35, 877—893. https://doi.org/10.1093/plankt/fbt028
Kotta, J., Lauringson, V., Martin, G., Simm, M., Kotta, I., Herkül, K., Ojaveer, H., 2008. Gulf of Riga and Pärnu Bay. In: Schiewer, U. (Ed.), Ecology of Baltic Coastal Waters. Springer, Heidelberg, Berlin, 217—243.
Kuhn, M., 2021. caret: Classification and Regression Training. R package version 6.0-90. https://CRAN.R-project.org/package=caret
Labucis, A., Purina, I., Labuce, A., Barda, I., Strake, S., 2017. Spring seasonal pattern of primary production in the Gulf of Riga (Baltic Sea) after a mild winter. Environ. Exp. Biol. 15, 247—255. https://doi.org/10.22364/eeb.15.26
Lancelot, C., Muylaert, K., 2011. 7.02 — Trends in Estuarine Phytoplankton Ecology. In: Wolanski, E., McLusky, D. (Eds.), Treatise on Estuarine and Coastal Science. Acad. Press, Waltham, 5—15. https://doi.org/10.1016/B978-0-12-374711-2.00703-8
Leles, S.G., Mitra, A., Flynn, K.J., Stoecker, D.K., Hansen, P.J., Calbet, A., McManus, G.B., Sanders, R.W., Caron, D.A., Not, F., Hallegraeff, G.M., Pitta, P., Raven, J.A., Johnson, M.D., Glibert, P.M., Våge, S., 2017. Oceanic protists with different forms of acquired phototrophy display contrasting biogeographies and abundance. Proc. Biol. Sci. B 284 (1860). https://doi.org/10.1098/rspb.2017.0664
Liland, K.H., Mevik, B.H., Wehrens, R., 2022. pls: Partial Least Squares and Principal Component Regression. R package version 2.8-1. https://CRAN.R-project.org/package=pls
Lindholm, T., Mörk, A.-C., 1990. Depth maxima of *Mesodinium rubrum* (Lohmann) Hamburger & Buddenbrock — examples from a stratified Baltic Sea inlet. Sarsia 75, 53—64. https://doi.org/10.1080/00364827.1990.10413441
Lips, I., Lips, U., 2017. The Importance of *Mesodinium rubrum* at Post-Spring Bloom Nutrient and Phytoplankton Dynamics in the Vertically Stratified Baltic Sea. Front. Mar. Sci. 4, 407. https://doi.org/10.3389/fmars.2017.00407
Lischka, S., Bach, L.T., Schulz, K.-G., Riebesell, U., 2017. Ciliate and mesozooplankton community response to increasing CO2 levels in the Baltic Sea: insights from a large-scale mesocosm experiment. Biogeosciences 14, 447—466. https://doi.org/10.5194/bg-14-447-2017
Malone, T.C., Chervin, M.B., 1979. The production and fate of phytoplankton size fractions in the plume of the Hudson River, New York Bight. Limnol. Oceanogr. 24, 683—696.
Menden-Deuer, S., Lessard, E.J., 2000. Carbon to volume relationships for dinoflagellates, diatoms, and other protist plankton. Limnol. Oceanogr. 45, 569—579. https://doi.org/10.4319/lo.2000.45.3.0569
Mevik, B.H., Wehrens, R., 2015. Introduction to the pls Package. Help Section of The "Pls" Package of R Studio Software, 1—23.
Mitra, A., Flynn, K.J., Burkholder, J.M., Berge, T., Calbet, A., Raven, J.A., Granéli, E., Glibert, P.M., Hansen, P.J., Stoecker, D.K., Thingstad, F., Tillmann, U., Våge, S., Wilken, S., Zubkov, M.V., 2014. The role of mixotrophic protists in the biological carbon pump. Biogeosciences 11, 995—1005. https://doi.org/10.5194/bg-11-995-2014
Mitra, A., Flynn, K.J., Tillmann, U., Raven, J.A., Caron, D., Stoecker, D.K., Not, F., Hansen, P.J., Hallegraeff, G., Sanders, R., Wilken, S., McManus, G., Johnson, M., Pitta, P., Våge, S., Berge, T., Calbet, A., Thingstad, F., Jeong, H.J., Burkholder, J., Glibert, P.M., Granéli, E., Lundgren, V., 2016. Defining Planktonic Protist Functional Groups on Mechanisms for Energy and Nutrient Acquisition: Incorporation of Diverse Mixotrophic Strategies. Protist 167, 106—120. https://doi.org/10.1016/j.protis.2016.01.003
Moeller, H.V., Johnson, M.D., Falkowski, P.G., 2011. Photoacclimation in the phototrophic marine ciliate *Mesodinium rubrum* (Ciliophora). J. Phycol. 47, 324—332. https://doi.org/10.1111/j.1529-8817.2010.00954.x
Montagnes, D.J.S., Allen, J., Brown, L., Bulit, C., Davidson, R., Díaz-Avalos, C., Fielding, S., Heath, M., Holliday, N.P., Rasmussen, J., Sanders, R., Waniek, J.J., Wilson, D., 2008. Factors controlling the abundance and size distribution of the phototrophic ciliate *Myrionecta rubra* in open waters of the North Atlantic. J. Eukaryot. Microbiol. 55, 457—465. https://doi.org/10.1111/j.1550-7408.2008.00344.x
Mousseau, L., Fortier, L., Legendre, L., 1998. Annual production of fish larvae and their prey in relation to size-fractionated primary production (Scotian Shelf, NW Atlantic). ICES J. Mar. Sci. 55, 44—57. https://doi.org/10.1006/jmsc.1997.0224

Nielsen, T.G., Kiørboe, T., 1994. Regulation of zooplankton biomass and production in a temperate, coastal ecosystem. 2. Ciliates. Limnol. Oceanogr. 39, 508—519.

Nishitani, G., Yamaguchi, M., 2018. Seasonal succession of ciliate *Mesodinium* spp. with red, green, or mixed plastids and their association with cryptophyte prey. Sci. Rep. 8, 17189. https://doi.org/10.1038/s41598-018-35629-4

Olenina, I., Hajdu, S., Edler, L., Andersson, A., Wasmund, N., Busch, S., Gobel, J., Gromisz, S., Huseby, S., Huttunen, M., Jaanus, A., Kokkonen, P., Ledaine, I., Niemkiewicz, E., 2006. Biovolumes and size-classes of phytoplankton in the Baltic Sea. Baltic Sea Environ. Proc. No 106. [https://epic.awi.de/30141/1/bsep106.pdf]

Olesen, M., Lundsgaard, C., Andrushaitis, A., 1999. Influence of nutrients and mixing on the primary production and community respiration in the Gulf of Riga. J. Marine Syst. 23, 127—143. https://doi.org/10.1016/S0924-7963(99)00054-8

Olli, K., Heiskanen, A.-S., Seppälä, J., 1996. Development and fate of *Eutreptiella gymnastica* bloom in nutrient-enriched enclosures in the coastal Baltic Sea. J. Plankton Res. 18, 1587—1604. https://doi.org/10.1093/plankt/18.9.1587

Omstedt, A., Edman, M., Claremar, B., Frodin, P., Gustafsson, E., Humborg, C., Hägg, H., Mörth, M., Rutgersson, A., Schurgers, G., Smith, B., Wällstedt, T., Yurova, A., 2012. Future changes in the Baltic Sea acid—base (pH) and oxygen balances. Tellus B Chem. Phys. Meteorol. 64, 19586. https://doi.org/10.3402/tellusb.v64i0.19586

Probyn, T.A., 1990. Size-fractionated measurements of nitrogen uptake in aged upwelled waters: Implications for pelagic food webs. Limnol. Oceanogr. 35, 202—210. https://doi.org/10.1093/plankt/fbh110

Purina, I., Labucis, A., Barda, I., Jurgensone, I., Aigars, J., 2018. Primary productivity in the Gulf of Riga (Baltic Sea) in relation to phytoplankton species and nutrient variability. Oceanologia 60 (4), 544—552. https://doi.org/10.1016/j.oceano.2018.04.005

R Core Team, 2019. R: A language and environment for statistical computing. R Foundation for Statistical Computing, Vienna, Austria.

Rychert, K., 2004. The size structure of the *Mesodinium rubrum* population in the Gdańsk Basin. Oceanologia 46 (3), 439—444. https://old.iopan.pl/oceanologia/463ryche.pdf

Sanders, R.W., 1995. Seasonal distributions of the photosynthesizing ciliates *Laboea strobila* and *Myrionecta rubra* (= *Mesodinium rubrum*) in an estuary of the Gulf of Maine. Aquat. Microb. Ecol. 9, 237—242.

Sin, Y., 2000. Seasonal variations of size-fractionated phytoplankton along the salinity gradient in the York River estuary, Virginia (USA). J. Plankton Res. 22, 1945—1960. https://doi.org/10.1093/plankt/22.10.1945

Skudra, M., Lips, U., 2017. Characteristics and inter-annual changes in temperature, salinity and density distribution in the Gulf of Riga. Oceanologia 59 (1), 37—48. https://doi.org/10.1016/j.oceano.2016.07.001

Sommer, U., Adrian, R., De Senerpont Domis, L., Elser, J.J., Gaedke, U., Ibelings, B., Jeppesen, E., Lürling, M., Molinero, J.C., Mooij, W.M., van Donk, E., Winder, M., 2012. Beyond the Plankton Ecology Group (PEG) Model: Mechanisms Driving Plankton Succession. Annu. Rev. Ecol. Evol. Syst. 43, 429—448. https://doi.org/10.1146/annurev-ecolsys-110411-160251

Sommer, U., Charalampous, E., Genitsaris, S., Moustaka-Gouni, M., 2016. Benefits, costs and taxonomic distribution of marine phytoplankton body size. J. Plankton Res. 39, 494—508. https://doi.org/10.1093/plankt/fbw071

Soria-Píriz, S., García-Robledo, E., Papaspyrou, S., Aguilar, V., Seguro, I., Acuña, J., Morales, Á., Corzo, A., 2017. Size fractionated phytoplankton biomass and net metabolism along a tropical estuarine gradient. Limnol. Oceanogr. 62, S309—S326. https://doi.org/10.1002/lno.10562

Spilling, K., Markager, S., 2008. Ecophysiological growth characteristics and modeling of the onset of the spring bloom in the Baltic Sea. J. Marine Syst. 73, 323—337. https://doi.org/10.1016/j.jmarsys.2006.10.012

Stoecker, D.K., Putt, M., Davis, L.H., Michaels, A.E., 1991. Photosynthesis in *Mesodinium rubrum*: species-specific measurements and comparison to community rates. Mar. Ecol. Prog. Ser. 73, 245—252.

Taylor, F.J.R., Blackbourn, D.J., Blackbourn, J., 1971. The Red-Water Ciliate *Mesodinium rubrum* and its "Incomplete Symbionts": A Review Including New Ultrastructural Observations. J. Fish. Res. Board Can. 28, 391—407.

Tong, M., Smith, J.L., Kulis, D.M., Anderson, D.M., 2015. Role of dissolved nitrate and phosphate in isolates of *Mesodinium rubrum* and toxin-producing *Dinophysis acuminata*. Aquat. Microb. Ecol. 75, 169—185. https://doi.org/10.3354/ame01757

Tremblay, J.-E., Legendre, L., 1994. A model for the size-fractionated biomass and production of marine phytoplankton. Limnol. Oceanogr. 39, 2004—2014. https://doi.org/10.4319/lo.1994.39.8.2004

Utermöhl, H., 1958. Zur Vervollkommnung Der Quantitativen Phytoplankton-Methodik. Mitt. Internat. Verein. Limnol. 9, 1—38.

Van Niel, C.B., 1949. The comparative biochemistry of photosynthesis. Am. Sci. 37, 371—383.

Wasmund, N., Andrushaitis, A., Łysiak-Pastuszak, E., Müller-Karulis, B., Nausch, G., Neumann, T., Ojaveer, H., Olenina, I., Postel, L., Witek, Z., 2001. Trophic status of the south-eastern Baltic sea: a comparison of coastal and open areas. Estuar. Coast. Shelf Sci. 53 (6), 1—16. https://doi.org/10.1006/ecss.2001.0828

Wasmund, N., Uhlig, S., 2003. Phytoplankton trends in the Baltic Sea. ICES J. Mar. Sci. 60, 177—186. https://doi.org/10.1016/S1054-3139(02)00280-1

Wassman, P., Tamminen, T., 1999. Pelagic eutrophication and sedimentation in the Gulf of Riga: a synthesis. J. Marine Syst. 23, 269—283. https://doi.org/10.1016/S0924-7963(99)00062-7

Wickham, H., 2009. ggplot2: Elegant Graphics for Data Analysis. Springer Science & Business Media.

Wilkerson, F.P., Grunseich, G., 1990. Formation of blooms by the symbiotic ciliate *Mesodinium rubrum*: the significance of nitrogen uptake. J. Plankton Res. 12, 973—989. https://doi.org/10.1093/plankt/12.5.973

Winder, M., Schindler, D.E., 2004. Climate change uncouples trophic interactions in an aquatic ecosystem. Ecology 85, 2100—2106. https://doi.org/10.1890/04-0151

Witek, M., 1998. Annual changes of abundance and biomass of planktonic ciliates in the Gdańsk basin, southern Baltic. Int. Rev. Hydrobiol. 83, 163—182. https://doi.org/10.1002/iroh.19980830207